# Unsteady temperature, heat transfer rate and HTF outlet temperature variation during charging of latent thermal energy storage unit

F. Benmoussa [1*], A. Benzaoui [2] and H. Benmoussa [1]

[1] Faculty of Technology, Mechanics Department,
University of Batna 2, 1 rue Chahid Boukhlouf, Batna 05000, Algeria
[2] Faculty of Physics, University of Sciences and Technology
Houari Boumedienne, USTHB
B.P. 32, 16111 Bab Ezzouar, Algeries, Algeria

(reçu le 25 Janvier 2019 - accepté le 28 Mars 2019)

**Abstract** - *This work reports a detailed numerical study that is aimed to determine the variation of the three principal parameters, temperature of two phase change materials (PCMs), heat transfer rate and heat transfer fluid (HTF) outlet temperature, during charging of latent thermal energy storage unit (LTES). The unit is consisting of a shell-and-tube type. The shell space is filled with two paraffin wax named PCM1 and PCM2. During charging process, hot fluid heats the PCMs, and when PCMs melts, the heat is stored. A mathematical model based on the conservation energy equations was developed and numerically investigated. Numerical results show that, the variation of the three principal parameters goes through three distinct periods. As time progress, the heat transfer rate increases, reaches its maximum value during the first period, and then decreases, until finally it equals zero. The HTF outlet temperature remains constant and is equal to its initial temperature for approximately 200 seconds. During this time period, the heat storage capacity is greater, PCM1 and PCM2 store energy in the sensible form only. The analysis and discussion of results are employed to evaluate the correspondence between the variations of the three parameters in term of charging time.*

**Résumé** - *Ce travail rapporte une étude numérique détaillée qui vise à déterminer les variations instationnaires de trois principaux paramètres, température des deux matériaux à changement de phase, le taux de transfert thermique et la température de sortie du fluide caloporteur, durant le processus de charge d'une unité de stockage thermique par chaleur latente. L'unité de stockage est constituée de deux tubes concentriques, l'espace annulaire est remplie de deux paraffines wax nommée PCM1 et PCM2. Durant le processus de charge, le fluide chaud chauffe le PCM, et quand le PCM se fusionne, la chaleur est stockée. Un modèle mathématique basé sur les équations de conservation d'énergie est développé. Les résultats numériques montrent que, les variations des trois principaux paramètres passent par trois périodes. Le taux de stockage thermique augmente, atteint une valeur maximal durant la première période, après il diminue, jusqu'à une valeur zéro. La température de sortie du fluide caloporteur reste constante est égale à sa température initiale pendant approximativement 200 seconds. Durant cette période le taux de stockage thermique est important, PCM1 et PCM2 stockent l'énergie par chaleur sensible. L'analyse et la discussion des résultats sont utilisées pour évaluer la correspondance entre les variations des trois paramètres en termes de temps et délais de stockage.*

**Keywords**: Thermal energy storage - Phase change materials - Heat transfer rate - HTF outlet temperature.

## 1. INTRODUCTION

Latent thermal energy storage systems (LTES) using phase change materials (PCMs) have attracted much attention over the past decades due to their high energy storage density and near isothermal phase transition during melting process [1].

* benmoussa_fouzi@yahoo.fr

The most widely investigated PCMs include paraffins, fatty acid and salt hydrates [2, 4]. The development of such systems involves a completely understanding the heat transfer mechanism in PCMs when they undergo solid to liquid phase transition in the required operating conditions. Also to control the variation of the principal parameters, especially temperature and heat transfer capacity.

There are many research studies focused on the development of the LTES unit filled with different PCMs. Among them, our paper published in the journal called: Case Studies in Thermal Engineering,

Benmoussa *et al.* [5] the research paper studied the effect of inlet temperature of HTF on the charging process of cascade latent thermal energy storage unit with two PCMs. An enhancement of 73.8 % was achieved when the HTF temperature is increased from 338 K to 353 K.

Seddegh *et al.* [6] investigated the effect of the operational and geometrical parameters on vertical cylindrical shell-and-tube LTES unit. Four different ratios of the shell-to-tube radius are considered. The average PCM temperature, liquid fraction, and stored energy are calculated to evaluate the performance of the storage unit. The results show that a shell to tube radius ratio of 5.4 offers better system performance in terms of charging time and stored energy. Moreover, the storage performance does not affected by the HTF flow rate; however, the charging time greatly affected by the HTF temperature.

Stritih [7] experimentally investigated the heat transfer characteristics of a LTES system with a finned surface using paraffin as PCM with low melting point for charging and discharging processes. The Nusselt number has been determined as a function of Rayleigh number and calculated the fin effectiveness. A reduction in the melt convection in PCM was observed with the presence of fin.

Ma *et al.* [8] investigated in detail the thermal performance of a high-temperature LTES system in concentrated solar power. The total charging/discharging time, average charging/discharging power and overall heat storage efficiency have been obtained by a series of experimental tests. The performance enhancement of the unit by using annular fins is also examined.

The results show that, the distribution of PCM temperature becomes more uniform and the maximum temperature difference in the PCM is greatly decreased with adding annular fins. Also, the average charging and discharging powers are, respectively, increased by 6.8 % and 9.1 %.

Very recently, Niyas *et al.* [9, 10] performed numerical and experimental analyses to evaluate the thermal performance of shelland-tube type LTES system with fins embedded in PCM. The results show that natural convection is significant during the charging process, whereas during discharging process, the conduction heat transfer is the dominant mode. The charging time is found to be less compared to the discharging time.

Gasia *et al.* [11] experimentally evaluate four different heat exchanger systems based on the shell-and-tube concept, in order to quantify and compare the influence of the addition of fins and the use of different HTF on the thermal performance. All experiments have been performed using paraffin RT58 as PCM and under the same boundary conditions and methodology. For the same HTF, results showed that finned designs showed an improvement of up to 40 %. On the contrary, for the same design, water yielded results up to 44 % higher.

In the present study, a physical and mathematical model based on the conservation energy equations was developed for the shell-and-tube LTES unit filled with two

paraffin wax named PCM1 and PCM2. Numerical simulations are carried out using Fluent 6.3 to evaluate the correspondence between different parameters. The variation of the three principal parameters, temperature of PCM1 and PCM2, heat transfer rate and HTF outlet temperature have been obtained by a series of numerical investigations and represented graphically.

## 2. PHYSICAL MODEL AND GOVERNING EQUATIONS

### 2.1 Physical model

The shell-and-tube PCMs storage unit considered in the present study is shown in figure 1**a**, which is similar to the model used by Lacroix [12]. It consists of an inner tube, an outer tube, and an annulus filled with PCM. However, the unit considered in this study is filled with two paraffin wax, named PCM1 and PCM2, having different melting temperatures (333 K and 323 K, respectively). The physical model to be analyzed is represented in figure 1**b**.

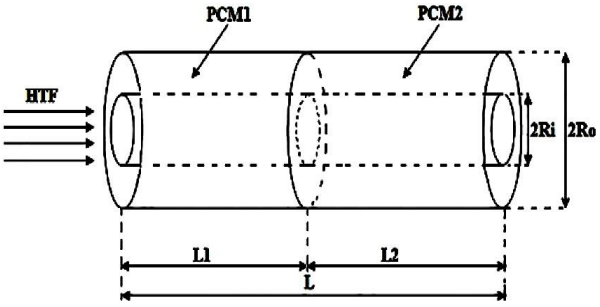


Fig. 1**a**: Schematic representation of the LTES unit with two PCMs

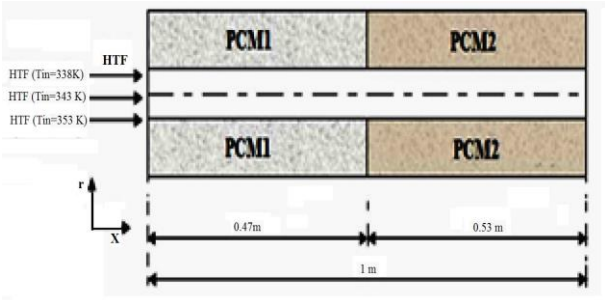


Fig. 1**b**: Physical model for numerical calculations

HTF (water) flows through the inner tube and exchanges heat with PCMs. During charging process, hot water circulates in the direction of the melting temperature increase. **Table 1** summarizes the thermo-physical properties of the HTF and PCMs. The dimensions of the unit are $L_1 = 0.47$ m, $L_2 = 0.53$ m, $R_i = 0.635$ cm, and $R_0 = 1.135$ cm. The HTF inlet velocity was maintained constant during the numerical tests to a value of 0.03 m/s.

**Table 1**: Thermo-physical properties of the HTF and PCMs:
Watanabe *et al.* [13], Yang *et al.* [14], Incropera *et al.* [15]

| | HTF | PCM1 | PCM2 |
|---|---|---|---|
| Fusion temperature, K | / | 333 | 323 |
| Density, kg/m$^3$ | 976 | 861 | 848 |

| | | | |
|---|---|---|---|
| Thermal conductivity, W/mK | 0.668 | 0.4 | 0.4 |
| Specific heat, J/kgK | 4.191 | 1,850 | 1.650 |
| Latent heat of fudion, kJ/kg | $3.34.10^2$ | $2.09.10^2$ | $2.00.10^2$ |
| Dynamic viscosity, kg/ms | $389.10^{-6}$ | $6.3.10^{-3}$ | $5.6.10^{-3}$ |

### 2.2 Assumptions

- The HTF is incompressible and can be considered as a Newtonian fluid;
- The flow is considered as laminar, unsteady, thus no turbulence model is required;
- The thermo-physical properties of the PCMs and HTF are independent of temperature;
- The initial temperature of the unit is uniform, the PCMs are in solid phase for the charging process and in liquid phase for the discharging process;
- The outer surface of the shell side is treated as an adiabatic boundary.

### 2.3 Mathematical formulations

The energy equations for the HTF and PCMs are shown as follows:

**a-** For the HTF region

$$(\rho C_p)_f\left(\frac{\partial T_f(x,r,t)}{\partial t}+U_f(r)\frac{\partial T_f(x,r,t)}{\partial x}\right)=k_f\left(\frac{\partial^2 T_f(x,r,t)}{\partial r^2}+\frac{1}{r}\frac{\partial T_f(x,r,t)}{\partial r}+\frac{\partial^2 T_f(x,r,t)}{\partial x^2}\right) \quad (1)$$

$x>0\ ;\ 0<r<R_i\ ;\ t<0$

Where $\rho$ is the density of fluid, $C_p$ the specific heat, $U$ the fluid velocity and $k$ the thermal conductivity.

**b-** For the PCMs region

$$(\rho C_p)_{pcm}\frac{\partial \theta_{pcm}(x,r,t)}{\partial t}=k_{pcm}\left(\frac{\partial^2 \theta_{pcm}(x,r,t)}{\partial x^2}+\frac{1}{r}\frac{\partial}{\partial r}\left(r\frac{\partial \theta_{pcm}(x,r,t)}{\partial r}\right)\right)-\rho_{pcm}\Delta H\frac{\partial f}{\partial t} \quad (2)$$

$x>0\ ;\ R_i<r<R_0\ ;\ t>0$

where: $\theta_{pcm}=(T-T_M)$ , $T_M=\begin{cases} T_{M1} & 0\le x\le L_1 \\ T_{M2} & L_1\le x\le L_2 \end{cases}$ (3)

$f$ is the PCMs melting fraction. The melting fraction during charging and discharging processes is determined as:

$$\left\{\begin{array}{lll} f=0 & \theta<0 & \text{Solid} \\ 0<f<1 & \theta=0 & \text{Solid+Liquid} \\ f=1 & \theta>0 & \text{Liquid} \end{array}\right\} \quad (4)$$

The {Eq. (2)} is formulated by using the enthalpy method Voller [16], in which the total enthalpy is split into sensible heat and latent heat:

$$H(T)=h(t)+\rho f\Delta H \quad (5)$$

Where: $h(T)=\int_{T_M}^{T}\rho C_p\,dt$ (6)

### 2.4 Initial and boundary conditions

**a-Initial conditions**

For the HTF region

$$\begin{cases} T_f\ (x, 0 < r < R_i\ ,\ t=0) = T_{f.ini} \\ U_f\ (x,\ 0 < r < R_i\ ,\ t=0) = U_{f.ini} \end{cases} \tag{7}$$

For the PCMs region

$$T_{PCM1} = T_{PCM2}\ (x,\ R_i \le r \le R_0\ ,\ t = 0) = 303\ K \tag{8}$$

**b-Boundary conditions**

For the HTF region

$$\begin{cases} T_f\ (x, 0 \le r \le R_i\ ,\ t=0) = T_{f.ini} \\ U_f\ (x,\ 0 \le r \le R_i\ ,\ t=0) = 0.03\ m/s \end{cases} \tag{9}$$

$$\left.\frac{\partial U_f\ (x,r,t)}{\partial r}\right|_{r=0} = \left.\frac{\partial T_f\ (x,r,t)}{\partial r}\right|_{r=0} = 0 \qquad x > 0\ \ t > 0 \tag{10}$$

For the PCMs region

$$\left.\frac{\partial \theta_{pcm}\ (x,r,t)}{\partial r}\right|_{r=R_0} = 0 \qquad x > 0\ \ t > 0 \tag{11}$$

$$\left.\frac{\partial \theta_{pcm1}\ (x,r,t)}{\partial x}\right|_{x=0} = \left.\frac{\partial \theta_{pcm2}\ (x,r,t)}{\partial x}\right|_{x=L} = 0 \qquad R_i < r < R_0\ ,\ t > 0 \tag{12}$$

$$k_{pcm1}\left.\frac{\partial \theta_{pcm1}\ (x,r,t)}{\partial x}\right|_{x=L_1} = k_{pcm2}\left.\frac{\partial \theta_{pcm2}\ (x,r,t)}{\partial x}\right|_{x=L1} \tag{13}$$

$$\theta_{pcm1}\ (x = L_1, r, t)_{PCM1} = \theta_{pcm2}\ (x = L_1, r, t)_{PCM2} \tag{14}$$

At the inner surface boundary

$$h_f\ (\theta_f - \theta(x, r = R_i\ , t)) = k_{pcm1}\left.\frac{\partial \theta_{pcm1}\ (x,r,t)}{\partial r}\right|_{x=R_i} \qquad x > 0,\ r = R_i\ ,\ t > 0 \tag{15}$$

Where $h$ is local convective heat transfer coefficient ($W/m^2K$).

## 3. NUMERICAL SOLUTION

Numerical computations are performed by adopting commercial CFD code Fluent 6.3, which employs the finite volume method described by Patankar [17] and uses the enthalpy-porosity technique for modeling the melting process.

The energy equations were discretized with the first order upwind scheme. The time integration has been performed fully implicitly and control volumes of a uniform size and constant time steps were used.

## 4. RESULTS AND DISCUSSION

### 4.1 Variation of the temperature of PCM1 and PCM2

The storing of thermal energy has been observed. PCM1 and PCM2 were initially in the solid phase; its temperature is set to 303 K. The variation of the temperature of PCM1 and PCM2 at different locations T1 (0.117, 0.007), T2 (0.235, 0.008), T3 (0.352, 0.010) in PCM2 and T4 (0.602, 0.007), T5 (0.735, 0.008), T6 (0.867, 0.010) in PCM1, for three different HTF inlet temperatures, are shown in figures 2**a**, 2**b** e t 2**c**..

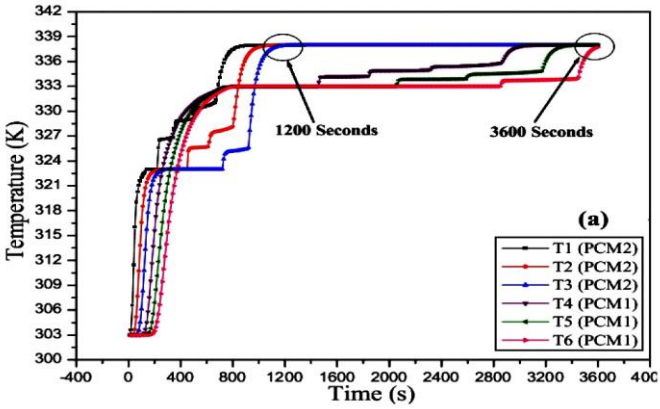


Fig. 2**a**: Variation of the temperature of PCM1 and PCM2 at some typical points **a-** $T_{f,in}$ = 338 K, b- $T_{f,in}$ = 343 K, and c- $T_{f,in}$ = 353 K

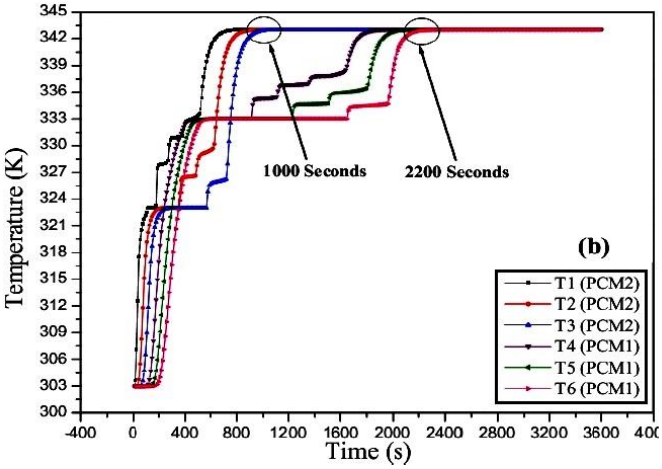


Fig. 2**b**: Variation of the temperature of PCM1 and PCM2 at some typical points a- $T_{f,in}$ = 338 K, **b-** $T_{f,in}$ = 343 K, and c- $T_{f,in}$ = 353 K

The heat transfer mechanism of the two PCMs shows three distinct periods for the change in temperature. The temperature of PCM1 and PCM2 during the first period increases rapidly from the start of heating process to the beginning of the phase change, corresponding to the melting point of each PCM ($T=333K$ for PCM1 and $T=323K$ for PCM2), each PCM stores energy primarily by sensible heat. During the second period, the energy is mainly charged by latent heat and the temperature of each PCM remains constant for a period of time.

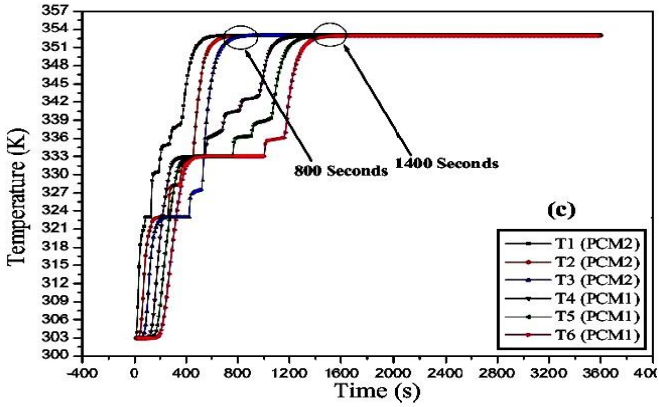


Fig. 2**c**: Variation of the temperature of PCM1 and PCM2 at some typical points
a- $T_{f,in}$ = 338 K, b- $T_{f,in}$ = 343 K, and **c-** $T_{f,in}$ = 353 K

At the third period, the temperature of each PCM starts to increase again, reaches its maximum value, then remains constant and equals to the HTF inlet temperature. The energy is charged only by sensible heat under a fusion form.

The time corresponding to the total melting time of each PCM, when the PCMs temperature reaches the inlet temperature of HTF are: For PCM2, 1200 s for $T_{f,in} = 338\,K$, 1000 s for $T_{f,in} = 343\,K$, 800 s for $T_{f,in} = 353\,K$. For PCM1, 3600 s for $T_{f,in} = 338\,K$, 2200 s for $T_{f,in} = 343\,K$, 1400 s for $T_{f,in} = 353\,K$.

As a conclusion, the melting rate of PCM2 is the fastest and that of PCM1 is the slowest, the low melting point of PCM2 plays an important role in the heat transfer mechanism. However, the PCM1 with high melting point defines the overall thermal behavior of the unit.

### 4.2 Variation of the heat transfer rate

For the same HTF inlet velocity, the variations of the heat transfer rate under different HTF inlet temperatures during charging process is shown in figure 3.

As time progress, the heat transfer rate increases, reaches its maximum value, and then decreases, until finally it equals zero. The variation of the heat transfer rate goes through three distinct periods. The time corresponding to the first period is about 200 seconds. The maximal value of the heat transfer rate increases nonlinearly.

For the HTF inlet temperature $T_{f,in} = 353\,K$, the maximal value is about 4000 W, but for $T_{f,in} = 343\,K$ and $T_{f,in} = 338\,K$ the maximal value is about 3150 W and 2650 W, respectively. The time corresponding to the second period depends on the HTF inlet temperature.

For HTF inlet temperature $T_{f,in} = 353\,K$, this time period is about 600 seconds, but for $T_{f,in} = 343\,K$ and $T_{f,in} = 338\,K$, this period is about 700 seconds and 1000 seconds, respectively. In the end of the second period, the heat transfer rate decreases to about 1625 W, 1300 W, and 600 W for $T_{f,in} = 353\,K$, $T_{f,in} = 343\,K$, and $T_{f,in} = 338\,K$, respectively.

At the third period, the heat transfer rate decreases further, reaches zero value, and then remains constant for the three different HTF inlet temperatures.

It can be seen that, the time corresponding to the end of the third period, correspond exactly to the period of time necessary for melting the PCM1 with high melting point (3600 s for $T_{f,in} = 338\,K$, 2200 s for $T_{f,in} = 343\ K$, 1400 s for $T_{f,in} = 343\ K$).

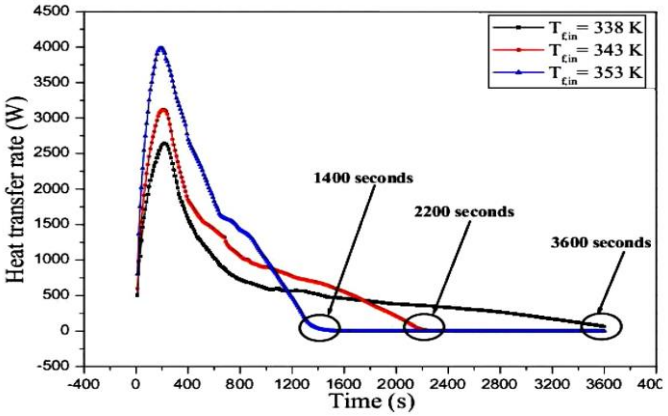


Fig. 3: Variation of the heat transfer rate during charging process

### 4.3 Variation of the HTF outlet temperature

The variations of the HTF outlet temperature during charging process for three different HTF inlet temperatures, under the same HTF inlet velocity is shown in figure 4.

As can be observed, the HTF outlet temperature remains constant for all HTF inlet temperatures and is equal to its initial temperature for approximately 200 seconds. During this time period, the heat storage capacity is greater. PCM1 and PCM2 store energy in the sensible form only.

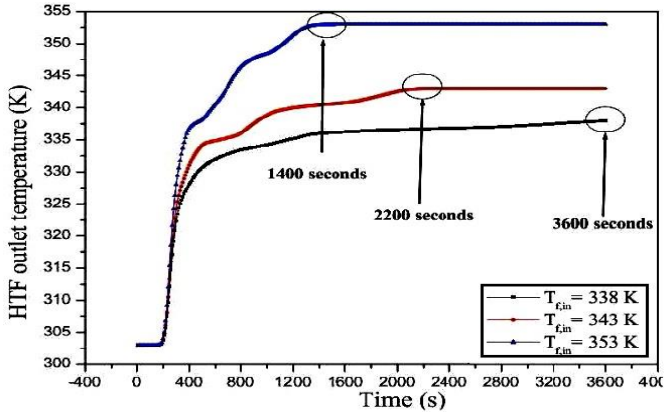


Fig. 4: Variation of the HTF outlet temperature during charging process

After 200 seconds, the second period starts and the HTF outlet temperature quickly increases over time. During this time period, the heat storage capacity reduces and the melting process is initiated. Then the HTF outlet temperature increase with lower change.

This is due to the fact that the melting process is more pronounced in the LTES unit. At the end of the charging process, the HTF outlet temperature remains constant and is equal to the HTF inlet temperature.

It can be seen that, the time corresponding to the end of the charging process, correspond exactly to the period of time necessary for melting the PCM1 with high melting point.

## 5. CONCLUSIONS

A mathematical model, based on the energy conservation equations was developed to predict the variation of the three principal parameters, temperature of two PCMs, heat transfer rate and HTF outlet temperature, during charging of LTES unit.

In order to analyze the correspondence between the three parameters, a variety of numerical tests were conducted.

According to the results and discussion, the following conclusions can be drawn:

**(01)** the variations of the three parameters goes through three distinct periods;

**(02)** the melting rate of  is the fastest and that of PCM1 is the slowest;

**(03)** the low melting point of PCM2 plays an important role in the heat transfer mechanism. However, the PCM1 with high melting point defines the overall thermal behavior of the unit;

**(04)** the time corresponding to the end of charging process, correspond exactly to the period of time necessary for melting the PCM;

**(05)** the heat transfer rate is large when the temperature difference between the HTF and the melting point of PCMs is large.

## NOMENCLATURE

| | |
|---|---|
| $C_p$ , Specific heat, J/kg.K | $h$ , Convective heat transfer coef., W/m$^2$.K |
| $L$ , Length of the tube, m | $k$ , Thermal conductivity, W/m.K |
| $R_i$ , Inner tube radius, m | $R_0$ , Outer tube radius, m |
| $T_{in}$ , Inlet temperature, K | $T_M$ , Melting temperature, K |
| $T$ , Temperature, K | $U_i$ , Inlet velocity, m/s |
| $f$ , PCMs melting fraction | $t$ , Time, s |
| $\rho$ , Density, kg/m$^3$ | $\Delta H$ , Latent heat of fusion, kJ/kg |
| $\theta_{PCM}$ , Relative temperature, K | $HTF$ , Heat transfer fluid |
| $LTES$, Latent thermal energy storage | $PCMs$ , Phase change materials |
| $f$ , Heat transfer fluid | $pcm$ , Phase change material |
| $in$ , Inlet boundary | $ini$ , Initial condition |

## REFERENCES

[1] R.K. Sharma, P. Ganesan, V.V. Tyagi and HSC. Metselaar, and S.C. Sandaran, '*Developments in organic solid liquid phase change materials and their applications in thermal energy storage*', Energy Conversion and Management, Vol. 95, pp. 193 - 228, 2015.

[2] M.M. Farid, A.M. Khudhair, S.A. Razack and S.A. Hallaj, '*A review on phase change energy storage: materials and applications*', Energy Conversion and Management, Vol. 45, pp. 1597 - 1615, 2004.

[3] A. Sharma, V.V. Tyagi, C. Chen and D. Buddhi, '*Review on thermal energy storage with phase change materials and applications*', Renewable and Sustainable Energy Reviews, Vol. 13, N°2, pp. 318 - 345, 2009.

[4] M.M. Kenisarin, '*Thermophysical properties of some organic phase change materials for latent heat storage. A review*', Solar Energy, Vol. 107, pp. 553 - 575, 2014.

[5] F. Benmoussa, A. Benzaoui, H. Benmoussa, '*Thermal behavior of latent thermal energy storage unit using two phase change materials: Effects of HTF inlet temperature*', Case Studies in Thermal Engineering, Vol. 10, pp. 475 - 483, 2017.

[6] S. Seddegh, X. Wang, M. Joybari, and F. Haghighat, '*Investigation of the effect of geometric and operating parameters on thermal behavior of vertical shell-and-tube latent heat energy storage systems*', Energy, Vol. 137, pp. 69-82, 2017.

[7] U. Stritih, '*An experimental study of enhances heat transfer in rectangular PCM thermal storage*', International Journal of Heat and Mass Transfer, Vol. 47, pp. 2841 - 2847, 2004.

[8] Z. Ma, W.W. Yang, F. Yuan, B. Jin and Y.L. He, '*Investigation on the thermal performance of a high-temperature latent heat storage system*', Applied Thermal Engineering, Vol. 122, N°25, pp. 579 - 592, 2017.

[9] H. Niyas, S. Prasad and P. Muthukumar, '*Performance investigation of a lab–scale latent heat storage prototype–numerical results*', Energy Conversion and Management, Vol. 135, pp. 188 - 199, 2017.

[10] H. Niyas, C.R.C. Rao and P. Muthukumar, '*Performance investigation of a lab-scale latent heat storage prototype–experimental results*', Solar Energy, Vol. 155, pp. 971 - 984, 2017.

[11] J. Gasia, J. Diriken, M. Bourke, J.V. Bael, and L.F. Cabeza, '*Comparative study of the thermal performance of four different shell-and-tube heat exchangers used as latent heat thermal energy storage systems*', Renewable Energy, Vol. 114, pp. 934 - 944, 2017.

[12] M. Lacroix, '*Numerical simulation of a shell-and-tube latent heat thermal energy storage unit*', Solar Energy, Vol. 50, pp. 357 - 367, 1993.

[13] T. Watanabe, H. Kikuchi, and A. Kanzawa, '*Enhancement of charging and discharging rates in a latent heat storage system by use of PCM with different melting temperatures*', Heat Recovery Systems and CHP, Vol. 13, pp. 57 - 66, 1993.

[14] L.Yang, X. Zhang, and G. Xu, '*Thermal performance of a solar storage packed bed using spherical capsules filled with PCM having different melting points*', Energy and Buildings, Vol. 68, pp. 639 - 646, 2014.

[15] F.P. Incropera, D.P. Dewitt, T.L. Bergman, and A.S. Lavine, '*Fundamentals of Heat and Mass Transfer*', 6th ed., Wiley, New York, 1996.

[16] V.R. Voller, '*Fast Implicit Finite-Difference Method for the Analysis of Phase Change Problems*', Numerical Heat Transfer, Vol. 17, pp. 155- 1 69, 1990.

[17] S.V. Patankar, '*Numerical Heat Transfer and Fluid Flow*', Hemisphere Publishing Corporation, New York, 1980.